Supplementary note on monochromatic $n \geq 4$ arm exponents for critical planar percolation

Gefei Cai

November 3, 2026

Note. *Starting from the proof for ξ_3 in [Cai26, Sections 2–6], the author discussed the extension to $n \geq 4$ with AI tools. Based on these discussions, AI tools then generated most of the proof for $n \geq 4$. Here we describe the result and outline the main ideas of the proof. The author takes full responsibility for the content of this note.*

We give the explicit operator in [Cai26, Theorem 1.4] and sketch the adaptation of the monochromatic three-arm case. Throughout, $\kappa = 6$, $n \geq 4$ and $d = n - 1$. We retain m for the inner quantum boundary length. Write $|x| = \sum_i x_i$, $\Delta_d = \{x \in (0,\infty)^d : |x| = 1\}$ and $dx = dx_1 \cdots dx_{d-1}$.

We use the cutting identities, computation of the LQG boundary-length kernel, renewal equations through Brownian annulus, estimates for the Mellin transform, and spectral threshold theorem developed in [Cai26, Sections 2–6]. The new steps concern connections from several marked points, simultaneous collisions of boundary marks, and cutting steps that leave some arc lengths unchanged. We state the corresponding extensions and sketch their proofs.

1 The explicit operator $\mathcal{L}_{n,\beta}$

For $0 < \beta < 1$, put $s(\beta) = (n + \beta)/2$ and $\theta_\beta = (5 - \beta)/4$. The operator in [Cai26, Theorem 1.4] acting on $L^1(\Delta_d, dx)$ is defined by

$$\mathcal{L}_{n,\beta} F := 2d\, \mathcal{A}_d \left[M_{\theta_\beta} \mathcal{T}_{n,s(\beta)} \left(\frac{\mathcal{A}_d F}{W_{\theta_\beta}} \right) \right]. \tag{1.1}$$

We now specify the averaging operator $\mathcal{A}_d$, the weights M_θ, W_θ, and the Mellin operator $\mathcal{T}_{n,z}$.

Averaging and weights. Let $\mathfrak{D}_d$ be the dihedral group acting on Δ_d generated by cyclic rotations and reversal of the coordinates. For $1 < \theta < 3/2$, set

$$\begin{aligned} (\mathcal{A}_d f)(x) &= \frac{1}{2d} \sum_{g \in \mathfrak{D}_d} f(gx), \\ M_\theta(x) = x_1^{-\theta} \prod_{i=2}^{d-1} x_i^{-1/2}, &\qquad W_\theta(x) = \sum_{g \in \mathfrak{D}_d} M_\theta(gx). \end{aligned} \tag{1.2}$$

The last coordinate of M_θ is unweighted. The factor $2d$ in (1.1) corresponds to the sum defining W_θ, whereas $\mathcal{A}_d$ is an average.

The Mellin operator $\mathcal{T}_{n,z}$. Let μ_n be the positive Borel measure on $(0,\infty)^{2d}$ obtained from the cutting sequences in Section 3, with X, Y denoting their initial and final ordered arc lengths. For

real $z < d$ and nonnegative measurable functions χ, f on Δ_d, define

$$\int_{\Delta_d} \chi(x)(\mathcal{T}_{n,z} f)(x)\,dx = \frac{1}{\Gamma(d-z)} \int e^{-|X|} \chi(X/|X|)|Y|^{-z} f(Y/|Y|)\,\mu_n(dX, dY). \tag{1.3}$$

The factor $\Gamma(d-z)$ comes from radial integration. Both sides may be infinite. For bounded χ and $f \in L^1(\Delta_d, W_\theta\,dx)$, the right-hand side converges absolutely on the strip in Proposition 4.1 and defines $\mathcal{T}_{n,z}$ for complex z.

The joint boundary-length measure μ_n. For Laplace variables $\mathbf{P}, \mathbf{Q} \in (0,\infty)^d$, the measure μ_n is characterized by

$$\mathcal{E}_n(\mathbf{P}; \mathbf{Q}) = \int e^{-\mathbf{P}\cdot X - \mathbf{Q}\cdot Y}\,\mu_n(dX, dY). \tag{1.4}$$

These transforms are finite and satisfy $\mathcal{E}_n(c\mathbf{P}; c\mathbf{Q}) = c^{-d}\mathcal{E}_n(\mathbf{P}; \mathbf{Q})$ for $c > 0$.

We have the following explicit expression for $\mathcal{E}_n$; see Proposition 3.1. Put $A_i = P_i^{3/2}$, $q = Q_d$, $k_0 = \sqrt{3}/(2\pi)$ and $\omega(du) = k_0 u^{2/3}\,du$. Then

$$\mathcal{E}_n(\mathbf{P}; \mathbf{Q}) = b_{d-1} + \int_{(0,\infty)^d} \mathcal{W}_q^{A_1}(v_1, v_d) \prod_{i=1}^{d-1} \mathsf{K}_{Q_i}(v_i, v_{i+1}) \prod_{i=1}^{d} \frac{\omega(dv_i)}{A_i + v_i}. \tag{1.5}$$

The functions $\mathsf{K}, \mathcal{W}, \mathcal{O}$ are given below. Starting from $f_1(v) = \mathcal{O}_q^{A_1, A_d}(v)/(A_1 + v)$ and $b_0 = 0$, the term b_{d-1} is determined by the recursion, for $1 \le h \le d-1$,

$$\begin{aligned} f_{h+1}(v) &= \frac{1}{A_{h+1} + v} \int_0^\infty \mathsf{K}_{Q_h}(u, v) f_h(u)\,\omega(du), \\ b_h &= \int_0^\infty f_{h+1}(v)\,\omega(dv) + \frac{b_{h-1}}{P_h + Q_h}. \end{aligned} \tag{1.6}$$

In the recursion for b_h, the integral gives the contribution from discarded boundary arcs containing exactly h inherited marks; see Section 2. The second term multiplies b_{h-1} by the Laplace transform factor $(P_h + Q_h)^{-1}$ for the surviving part of an inherited arc. For $h = d-1$, the factor $\mathcal{W}_q^{A_1}(v_1, v_d)$ couples the first and last integration variables, giving the cyclic integral in (1.5).

The kernel K_q. For $q, u, v > 0$,

$$\begin{aligned} \mathsf{K}_q(u, v) &= \frac{v^{2/3} - u^{2/3} + (u^{2/3} + v^{2/3} - q)\{\Upsilon(u^{1/3}/\sqrt{q}) - \Upsilon(v^{1/3}/\sqrt{q})\}}{v^2 - u^2} \\ &= \int_0^\infty \frac{B^{2/3} + u^{2/3} + v^{2/3}}{(q + B^{2/3})(B + u)(B + v)(u + v)}\,\omega(dB), \end{aligned} \tag{1.7}$$

where

$$\Upsilon(t) = \frac{\frac{3\sqrt{3}}{4} t^3 - t^2 - t^4 - \frac{3\sqrt{3}}{2\pi} t^6 \log t}{1 + t^6}. \tag{1.8}$$

The integral representation gives positivity, symmetry and the diagonal values. Coincident arguments in all these formulas are interpreted by continuity.

The endpoint functions $\mathcal{W}_q^A$ and $\mathcal{O}_q^{A,R}$. Put $J_q(u, a) = (u + a)\mathsf{K}_q(u, a)$. The first endpoint function is

$$\mathcal{W}_q^A(u, v) = \frac{J_q(u, A) - J_q(u, v)}{v - A}. \tag{1.9}$$

For the second, put $a = A^{1/3}$, $c = R^{1/3}$, $e = u^{1/3}$ and $q_2(x, y) = x^2 + xy + y^2$, where $A, R, u > 0$. Then

$$\begin{aligned} \mathcal{O}_q^{A,R}(u) &= \frac{3k_0}{(q+c^2)(a+c)}\,\mathfrak{I}(R_1 + R_2), \\ R_1(y) &= \frac{y^4\{ac + (a+c)y\}}{(a+y)q_2(c,y)(q+y^2)(e^3+y^3)}, \\ R_2(y) &= \frac{y^4\{ac + (a+c)y\}(e+y)}{(c+y)q_2(a,y)q_2(e,y)(y^4 - qy^2 + q^2)}. \end{aligned} \tag{1.10}$$

Here $\mathfrak{I}$ evaluates a rational integral: for $H(y) = \sum_p \sum_{j=1}^{m_p} c_{p,j}(y-p)^{-j} = O(y^{-2})$ with no pole on $[0, \infty)$,

$$\mathfrak{I}(H) = \int_0^\infty H(y)\,dy = \sum_p \left\{ -c_{p,1}\log(-p) + \sum_{j=2}^{m_p} \frac{c_{p,j}(-p)^{1-j}}{j-1} \right\}. \tag{1.11}$$

Here p ranges over the poles of H, m_p is the order of the pole, and $c_{p,j}$ are the partial-fraction coefficients; the logarithm is principal. Both endpoint functions are positive; they are obtained by integrating the boundary-length measures in Proposition 3.1.

Remark 1.1 (Numerical evaluation of ξ_n for $n \geq 4$). We use a collocation discretization of $\mathcal{L}_{n,\beta}$ in (1.1), combined with numerical quadrature, to obtain a finite matrix. Solving for the value of β at which its spectral radius is one gives an estimate of β_n, and [Cai26, (1.7)] then gives an estimate of ξ_n. For u close to v, the positive integral representation in (1.7) evaluates $\mathsf{K}_q(u, v)$ without subtractive cancellation.

For ξ_3, the computation in [Cai26, Appendix A.3] uses one-dimensional quadrature with the elementary kernel in [Cai26, (1.3)]. For $n \geq 4$, the eigenfunction depends on $d - 1 = n - 2$ independent coordinates in Δ_d. The number of unknowns in a tensor-product discretization with N points per coordinate is of order N^{n-2}, compared with order N in the three-arm case. The Laplace transform of μ_n in (1.5) also contains a cyclic integral in $d = n - 1$ variables. Several normalized arc lengths x_i can approach zero simultaneously, requiring refinement near intersections of boundary faces of Δ_d. Cutting sequences that leave an arc length unchanged give singular contributions to μ_n, supported where the corresponding coordinates of X and Y agree. Obtaining precision comparable to that for ξ_3 is therefore substantially more costly, as it requires refinement in several variables, accurate evaluation of the singular contributions, and control of discretization, quadrature and truncation errors and their propagation to β_n and ξ_n.

2 The connection event and the cutting identity

To construct μ_n, we extend the two-point boundary observable of [Cai26, Section 2] to a finite set M of boundary marks, with D, K and X_C as defined there. Let $H_j = H_j(D, K)$ be the continuum event of j black arms, with the black boundary conditions and inner-boundary approximation of [Cai26, Section 2.1]. Conditional on the field, sample the marks according to normalized quantum boundary length before imposing the percolation event. Define the connection event $G(D, K; M)$, abbreviated $G(M)$, using the path convention of [Cai26, Section 2]: for each $i \in M$, require two black paths from i and one from every other mark to distinct inner-boundary points, disjoint except that the two paths starting at i share their initial point. The paths may be chosen separately for each i, in the same configuration.

For $\mathbf{b} = (b_i)_{i\in M} \in \mathbb{Z}_{\geq 0}^M$, let $P_{\mathbf{b}}$ indicate the existence of $\sum_{i\in M} b_i$ simple black lattice paths, exactly b_i starting at each $i \in M$, each stopped at its first visit to the inner boundary. The paths

are vertex-disjoint except at common starting points, and each path meets M only at its starting point. For $S \subset M$, let $\lambda(S)$ be the maximum number of such paths starting in S, with the full marked set M kept fixed. Write $\mathbf{1}_M = (1)_{i\in M}$, and let e_i be the ith coordinate vector.

Lemma 2.1. *For finitely many fixed vectors* $\mathbf{b}$*, the lattice indicators* $P_{\mathbf{b}}$*, also with specified points forbidden to all paths, converge jointly as the mesh tends to zero. Almost every mark under quantum boundary length has at most two disjoint macroscopic black paths. At these marks,*

$$G(M) = \prod_{i\in M} P_{\mathbf{1}_M + e_i} = \mathbf{1}\{\lambda(S) \geq |S| + 1 \text{ for every } \varnothing \neq S \subset M\}. \tag{2.1}$$

For $|M| = d$*, this event implies* H_n*; for two marks, it is the observable [Cai26, (2.4)] and its continuum limit* $G(D, K; p, q)$*.*

Proof sketch. We extend the contact comparison of [Cai26, Section 2.1] to finitely many prescribed path counts. Failure to connect the prescribed N paths gives a separating configuration with at most $N-1$ black vertices, white paths and any required separating circuits. Pass these configurations to the limit, keeping each white path in its corresponding white cluster and preserving the prescribed sides and the marks and boundary components separated by the configuration, using [DMMY26, Lemma 2.7 and Proposition 3.1]. Errors away from marks force six bulk arms of type $BBWBBW$ or, after removing the black boundary row, three boundary arms with free boundary conditions. Their exponents $35/12$ and 2 make the union bounds vanish; bounded defects introduce only logarithmic factors [Nol08, Section 4.5]. Follow the approximation order of [Cai26, Section 2.1]: first let the mesh tend to zero with the boundary approximations and contact neighborhoods fixed, then remove these approximations and neighborhoods, and finally the interface-diameter cutoff. Boundary one-arm estimates exclude nontrivial white-cluster contacts and a third black path at sampled marks. On the lattice, the first equality in (2.1) follows from the definitions, and the second follows from the max-flow min-cut theorem with the marked set M fixed. Each condition on $\lambda(S)$ is a finite union of events $P_{\mathbf{b}} = 1$, so joint convergence gives the same identities in the limit. Separators between the boundary components avoid these marks, so the prescribed n paths imply H_n. □

Fix a set O of $d-1$ boundary marks with $G(O) = 1$. Consider open boundary arcs containing exactly h marks of O, cut off from K by finite separating configurations with $h+1$ distinct black vertices in the lattice approximation using a *minimal* number h of white clusters in $D \setminus K$, $1 \leq h \leq d-1$. Let $\mathcal{J}_O$ be the connected components of their union. For each fixed configuration, adjoin arbitrary finite collections of compact white paths in the same clusters, filling enclosed regions disjoint from K. Take the relative closure in $\overline{D} \setminus K$ of the union of the resulting discarded regions, retaining original outer prime ends. The path conditions are checked before taking this closure, with the prescribed sides retained; limiting contacts on K do not create additional exits.

Let A be such a region formed from h white clusters C in D with $\Pi_C(X_C) \cap K = \varnothing$, and put $I = O \cap A$, $|I| = h \geq 1$. Let U be the retained component containing K and $Q = \{q_0, \ldots, q_h\}$ the distinct exits from A to U, in boundary order. The exits are distinct points in the completion with their prescribed sides; their planar images may coincide. Let $C_A(I; Q)$ be the indicator that, for each $i \in I$, there are two black paths from i and one from every other mark of I to the $h+1$ distinct exits, stopped at their first exits and disjoint except that the two paths starting at i share their initial point. The paths may be chosen separately for each i, in the same configuration. Let $F_O(A)$ assert that its discarded arc belongs to $\mathcal{J}_O$ and A is the *largest* among all such regions with that arc. Put

$$E_O(p, q) = P_{\mathbf{1}_{O\cup\{p,q\}}}\, G(\{p, q\})G(O), \qquad p, q \notin O.$$

On H_n, the boundary partition consists of $\mathcal{J}_O$ and maximal single-cluster discarded arcs outside their union. Choose p as the next starting mark and q as its neighbor in a fixed orientation. Let Ψ, E be the Brownian annulus measure with independent CLE_6 and respectively $d, d+1$ ordered outer marks, integrated against quantum boundary length and weighted by G, E_O. Starting from $O \cup \{x\}$, let $\mathcal{B}$ describe cutting the first complete boundary-touching loop. Subsequently, $\mathcal{R}$ removes the region whose discarded arc contains no mark of O, retaining E_O, whereas $\mathcal{F}_h$ removes one whose arc contains h such marks. The terms Θ_0, Θ_1 record steps at which the white clusters meet K. Figure 1 shows the first step and the three subsequent alternatives, together with the numbers of marked points.

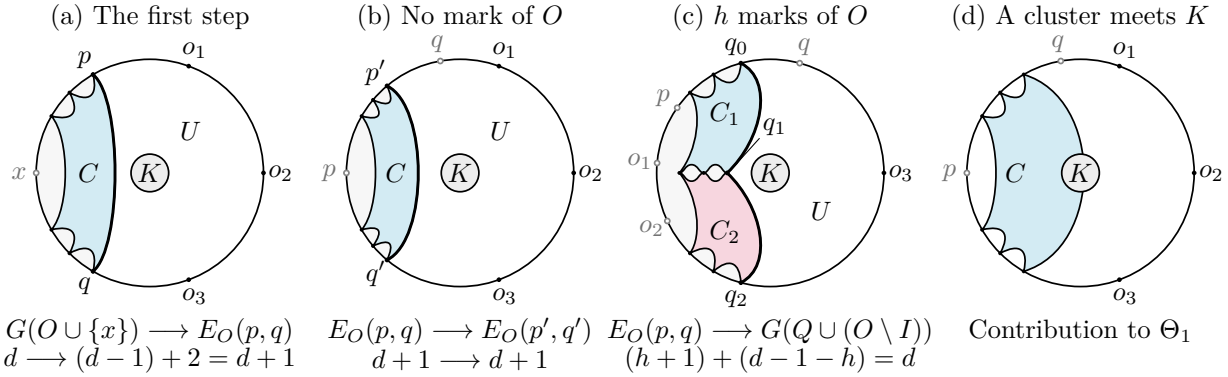


Figure 1: The cutting steps for $d = 4$ and $O = \{o_1, o_2, o_3\}$, with $h = 2$ in (c). Blue and pink indicate distinct white clusters; pale regions are discarded, and thick curves are newly exposed boundary arcs. Unlabeled dots are contacts, not additional marks; gray points cease to be marked. In (a), one mark is replaced by two exits. In (b), the discarded arc contains no mark of O, and the new exits replace both p and q, including q outside that arc. In (c), $h+1$ exits and $d-1-h$ inherited marks yield the event G with d marks, together with the indicator $C_A(I;Q)$ in (2.2). The factor $P_{\mathbf{1}_{O\cup\{p,q\}}}$ in E_O prescribes one path from each of its $n = d+1$ marks. A cluster meeting K contributes to Θ_1 in (d), or to Θ_0 at the first step.

Proposition 2.2 (Cutting identities)**.** *On $H_n \cap \{G(O) = 1\}$, the union of $\mathcal{J}_O$ agrees, up to quantum boundary-length null sets, with $\{p \notin O : G(O \cup \{p\}) = 0\}$. Each arc in $\mathcal{J}_O$ containing h marks of O has a largest region formed from h white clusters in D avoiding K, unless a chain of at most h white clusters in $D \setminus K$ reaches K. In the former case it has $h+1$ exits. For each fixed region A of the specified kind,*

$$\mathbf{1}_{H_n} G(O) \mathbf{1}_{F_O(A)} = C_A(I;Q)\, G\big(U, K; Q \cup (O \setminus I)\big). \tag{2.2}$$

The event in U has $h+1+(d-1-h) = d$ marks. For almost every choice of the distinct marks in $O \cup \{p,q\}$ with respect to the product of quantum boundary-length measures, on $H_n \cap \{G(O) = 1\}$, $E_O(p,q) = 1$ if and only if p, q lie in different partition classes. Consequently,

$$\Psi = \mathcal{B}\mathsf{E} + \Theta_0, \qquad \mathsf{E} = \mathcal{R}\mathsf{E} + \sum_{h=1}^{d-1} \mathcal{F}_h \Psi + \Theta_1. \tag{2.3}$$

After J substitutions the remainder is $\mathcal{B}\mathcal{R}^J\mathsf{E}$.

Proof sketch. Extend [Cai26, Lemma 2.5 and Proposition 2.3], applying [Cai26, Lemma 2.4] when cutting along each complete interface loop. The additional step enlarges the discarded regions using

the same white clusters and retaining the marked points and prescribed sides. Comparing the numbers of black vertices in separators for unions and intersections of overlapping discarded regions gives the maximal arcs; adjoining paths and taking unions gives the largest regions or a chain to K. Clusters avoiding K are cut successively in the order of their connecting paths.

For (2.2), failure of a required connection in U gives a separator which, joined to A, enlarges the discarded arc or region, or separates the two boundary components with at most $n-1$ black vertices, contradicting H_n. Conversely, deleting one exit reduces by at most one the maximum number of paths from any subset of I to distinct exits, under the preceding path rules. Thus $C_A(I;Q)$ supplies disjoint paths, one from each mark of I, avoiding whichever exit is needed on the retained side. The paths can therefore be joined at their first exits. To obtain H_n, separate the two paths from a marked exit of the retained component by moving one start to a nearby point on the inherited arc. Join the paths across the exits, then separate the two starts at the corresponding mark in I. This gives n distinct original outer endpoints, preserving their boundary order and disjointness in the lattice approximation. Lemma 2.1 passes these statements to the continuum. The same separation argument gives paths whose only possible intersections occur at their starting points. If one path passes through the starting point of another, there are three disjoint macroscopic black arms at that mark. Lemma 2.1 excludes this for almost every choice of the marks, giving the criterion for E_O. Removing the region associated with the class containing p gives another event E_O, the event G in (2.2), or a chain reaching K. These alternatives give $\mathcal{R}$, $\mathcal{F}_h$ and Θ_1, respectively. Starting from G, cutting the first loop gives E_O or a cluster meeting K, corresponding to $\mathcal{B}$ and Θ_0. Integration yields (2.3); finite substitution gives the stated remainder, whose vanishing is proved in Proposition 4.2. □

3 The joint boundary-length measure

We iterate the single-loop measure decomposition of [Cai26, Lemma 3.1 and Proposition 3.2], retaining all ordered marks and imposing the required connection events. A sequence $\mathcal{B}, \mathcal{R}^j, \mathcal{F}_h$, with $j \geq 0$ and $1 \leq h \leq d-1$, takes an event G to another event of the same form. Denote its initial and final arc lengths by X, Y, in the fixed boundary order used in (1.6). The calculation uses the following function of $a, b > 0$:

$$\mathsf{U}(a,b) = \frac{a^{2/3} - b^{2/3}}{a-b} = \frac{a^{1/3} + b^{1/3}}{a^{2/3} + (ab)^{1/3} + b^{2/3}}.$$

Proposition 3.1 (The joint boundary-length measure)**.** *Summing over these sequences gives the measure μ_n in (1.4). Its Laplace transform is (1.5), with separate variables $\mathbf{P}, \mathbf{Q}$ for every initial and final arc length, and its Mellin transform is (1.3).*

Proof sketch. Apply [Cai26, Lemma 3.1] before imposing the connection and maximality conditions, retaining the exterior data and the same unnormalized ordered marking measure on both sides. Conditional on the undecorated quantum surfaces, their boundary lengths and the preceding exterior data, distinct ordinary disks carry independent CLEs. Impose the connection events and maximality before integrating out these CLEs; connections and prescribed sides are preserved by [Cai26, Lemma 2.4]. Before these restrictions, new endpoints and surviving marks carry ordered quantum boundary-length marking. Tonelli's theorem preserves almost-sure assertions at these marks through finite cutting sequences, without resampling endpoints. The cutting identity in [Cai26, Proposition 3.2], the quantum-disk exploration law [GM18], and the stable resolvent formula [KKR13] give the joint length measures, including the length factors from ordered marking.

For $a, B, v > 0$, the Stieltjes identity is

$$\mathsf{U}(a,B)\mathsf{U}(a,v) = \int_0^\infty \frac{B^{2/3}+v^{2/3}+u^{2/3}}{(a+u)(B+u)(v+u)}\,\omega(du). \tag{3.1}$$

The Laplace transform gives (1.7), and successive divided differences give (1.6). Evaluating the endpoint integrals gives (1.9) and (1.10). For $h = d-1$, the joint restriction at both ends produces the cyclic term in (1.5), coupling the first and last integration variables. Tonelli's theorem allows summation over finite sequences; uniqueness of the Laplace transform identifies μ_n, and radial integration gives (1.3). □

Let L be the outer perimeter and $x \in \Delta_d$ the normalized successive arc lengths. For fixed x, write $z_d(L,x;m)\,dL\,dm$ for the Brownian annulus measure weighted by G, averaged over a cyclic starting mark sampled from normalized quantum boundary length. After integrating d ordered marks against unnormalized quantum boundary length, let $Z_d(\ell;m)$ be its density with respect to $d\ell_1\cdots d\ell_d\,dm$, where $\ell = Lx$. On a cylinder of modulus τ, let $\overline{G}_{n,\tau}(x)$ be the same starting-mark average with prescribed normalized quantum arc lengths x. Write Z_o, Z_i for the boundary masses of the lateral field of [Cai26, Section 5]. The expectations below are over the field and the independent CLE. Similarly, we have

Lemma 3.2. *The marked density and its Mellin transform satisfy*

$$Z_d(Lx;m) = L\,z_d(L,x;m), \qquad \int_0^\infty m^{-s} Z_d(Lx;m)\,dm = L^{-s}\Phi_s(x). \tag{3.2}$$

For $\gamma = \sqrt{8/3}$,

$$\Phi_s(x) = \frac{\sqrt{2}}{\gamma}\int_0^\infty \eta(2i\tau)e^{2\pi s^2\tau/3}\,\mathbb{E}\Big[(Z_o/Z_i)^s\overline{G}_{n,\tau}(x)\Big]\,d\tau. \tag{3.3}$$

For real s these are identities of nonnegative quantities, allowing $+\infty$.

Proof sketch. Dividing the marking factor L^d by the Jacobian L^{d-1} for $\ell = Lx$ gives the first identity in (3.2); homogeneity gives the second. By [Cai26, Lemma 4.2], cutting a loop disjoint from the filled metric ball preserves the ball and its boundary measure. The Brownian annulus construction [Cai26, (4.6)] and integration over the additive field constant in [Cai26, (5.7)] give (3.3). □

4 Boundary estimates and the renewal equation

The renewal equation adapts [Cai26, Proposition 4.3]; its integrability and the bound on the inhomogeneous term extend [Cai26, Propositions 5.1–5.3]. We first state the operator bounds needed for the spectral argument of [Cai26, Section 6].

For $1 < \theta < 3/2$, use the weighted space $L^1(\Delta_d, W_\theta\,dx)$ and operator

$$\mathcal{K}_{\theta,z} f = \frac{2d}{W_\theta}\mathcal{A}_d[M_\theta \mathcal{T}_{n,z}(\mathcal{A}_d f)].$$

Multiplication by W_θ is an isometry from $L^1(\Delta_d, W_\theta\,dx)$ onto $L^1(dx)$, and

$$\mathcal{L}_{n,\beta} = W_{\theta_\beta}\mathcal{K}_{\theta_\beta,s(\beta)}W_{\theta_\beta}^{-1}. \tag{4.1}$$

These operators have the same spectrum. We provide the following bound for $\mathcal{K}_{\theta,z}$. Set

$$a_\theta = \frac{d+2}{2} - \theta, \qquad c_\theta = \frac{3}{4\sin^2(2\pi(2-\theta)/3)} < 1.$$

Proposition 4.1. *Fix $1 < \theta < 3/2$. The family $\mathcal{K}_{\theta,z}$ is holomorphic in operator norm on $a_\theta < \Re z < a_\theta + 1$, is positive for real z, and satisfies*

$$\|\mathcal{K}_{\theta,a_\theta+it}\| \le c_\theta \quad (t \in \mathbb{R}), \qquad r_{\mathrm{ess}}(\mathcal{K}_{\theta,z}) \le c_\theta \quad (a_\theta \le \Re z < a_\theta + 1).$$

Here r_{ess} denotes the essential spectral radius, and all norms are operator norms on $L^1(\Delta_d, W_\theta\, dx)$. For every compact subset J of this half-closed strip, with $B_\varepsilon = \{x : \min_i x_i < \varepsilon\}$ and $\mathbf{1}_{B_\varepsilon}$ denoting multiplication by its indicator,

$$\lim_{\varepsilon \downarrow 0} \sup_{z \in J} \|(\mathcal{K}_{\theta,z} - \mathcal{K}_{\theta,a_\theta})\mathbf{1}_{B_\varepsilon}\| = 0. \tag{4.2}$$

For real z in the open strip, the kernel has a component with strictly positive density between almost every pair of interior points of Δ_d.

Proof sketch. At a_θ, summing over all possible final values of h cancels the inverse square-root weights of the inherited arcs that are shortened. Integration in the original boundary-length variables gives the norm bound c_θ. For other parameters, normalize the retained perimeter to one and estimate the resulting power of the original perimeter. Using the restrictions at both endpoints in the final step, we obtain a bound uniform in h and hence boundedness on $L^1(\Delta_d, W_\theta\, dx)$.

Near the boundary of the simplex, the weighted integrals concentrate where the original and retained perimeters agree. Moment bounds for the total length removed and the newly exposed arcs give (4.2), first for the arc carrying the power θ, and then for every boundary face by dihedral averaging. The estimates include simultaneous and nested collisions of marks. In each iterate of the operator, separate cutting sequences that change every original arc length from those leaving one unchanged. For the former, the corresponding changes of variables have full rank and give compact operators after truncation away from the boundary. For the latter, perimeter factors telescope and the contraction at a_θ applies. Together with (4.2), this gives the essential spectral radius bound. The operator $\mathcal{K}_{\theta,z}$ need not itself be compact. □

We next establish the renewal equation for Φ_s. Put $\sigma_n = \sqrt{1/4 + 3\xi_n}$. The bounds of [BN11] give $n/2 < \sigma_n < (n+1)/2$. Let $\Theta_{\theta,s}$ be obtained from $\Theta_0 + \mathcal{B}\sum_{j\ge 0}\mathcal{R}^j\Theta_1$ by the Mellin transform and the same weighted averaging as in $\mathcal{K}_{\theta,s}$.

Proposition 4.2 (Renewal equation)**.** *If $n/2 < s < \sigma_n$ and $1 < \theta < (n+3)/2 - s$, then $\Phi_s \in L^1(\Delta_d, W_\theta\, dx)$ and*

$$\Phi_s = \Theta_{\theta,s} + \mathcal{K}_{\theta,s}\Phi_s, \qquad \Theta_{\theta,s} \ge 0. \tag{4.3}$$

As $s \uparrow \sigma_n$,

$$\int_{\Delta_d} \Phi_s(x)\, dx \asymp \frac{1}{\sigma_n^2 - s^2}. \tag{4.4}$$

For every fixed $1 < \theta < (n+3)/2 - \sigma_n$, the norms $\|\Theta_{\theta,s}\|_{L^1(\Delta_d, W_\theta\, dx)}$ remain bounded in a neighborhood of σ_n.

Proof sketch. Arm separation compares the simplex integral of the expectation in (3.3) with the n-arm probability, as in [Cai26, Proposition 5.3]. Quasi-multiplicativity makes it comparable to $e^{-2\pi\xi_n\tau}$, giving (4.4). As k marks approach one another, the two outermost paths may use the black boundary row, leaving $k-1$ interior paths with half-plane exponent $k(k-1)/6$. After the Gaussian change of measure, use negative moments of orders $r_i \ge 0$ for the boundary masses near these marks and put $A = \sum_{i=1}^k (1 - r_i)$. The relevant integrability calculation is

$$\zeta(A) + \frac{k(k-1)}{6} - 1 = \frac{2}{3}\left(\frac{k+2}{2} - A\right)\left(A + \frac{k-3}{2}\right), \qquad \zeta(A) = \frac{5A - 2A^2}{3}.$$

Splitting the power θ between the endpoints of the first arc and adding one auxiliary boundary mark, with no extra arm, gives the stated range of θ. Negative moments of every order [RZ20, Corollary 1.2], together with covariance comparison, control small boundary masses. At small modulus, the common Gaussian factor cancels against the inner boundary mass as in [Cai26, (5.17)].

To remove the remainder in (2.3), forget all marks except p, q, which bounds E_O by the three-arm observable. Choose $3/2 < s_0 < \sigma_3 = \sqrt{1/4 + 3\xi_3}$; the square-root boundary bound at unit outer perimeter follows from [Cai26, Proposition 5.1]. Write a for the unnormalized quantum arc length between p, q and ℓ_0 for an unchanged arc length between two consecutive other marks. The comparison function $\sqrt{a}\,\ell_0^{-s_0-1/2}$ is homogeneous of degree $-s_0$ and locally bounded on compact subsets of the normalized simplex. Conjugating the corresponding unnormalized length kernel by $\sqrt{a}$ gives an auxiliary killed chain. Until killing, the log-ratio of the length of the adjacent arc shortened by $\mathcal{R}$ to a is bounded above by a centered, nondegenerate finite-variance random walk. Whenever this walk enters a fixed lower half-line, the conditional probability that the chain is killed at the next step is bounded below by a positive constant. Recurrence therefore makes the survival probability tend to zero. Exhaustion by compact sets in the normalized arc lengths and both perimeters makes the remainder measures tend to zero; Tonelli's theorem then permits the Mellin weights in (4.3).

For the inhomogeneous term, the first white cluster meeting K completes a chain of at most n white clusters from the outer boundary to K. Together with H_n, this gives $n+1$ polychromatic arms with defects at the at most $n-1$ contacts between consecutive white clusters. As in [Cai26, Proposition 5.2], the gap $\alpha_{n+1} = n(n+2)/12 > \xi_n$ absorbs the resulting polynomial factor in the modulus [SW01, Nol08]. □

5 Identification of the spectral threshold

Propositions 4.1 and 4.2 allow the spectral argument of [Cai26, Section 6] to be adapted for fixed θ.

Proposition 5.1 (Spectral threshold)**.** *Fix $1 < \theta < (n+3)/2 - \sigma_n$ and put $a = a_\theta$, $c = c_\theta$. Then $r(\mathcal{K}_{\theta,\sigma_n}) = 1$, and the eigenvalue one is algebraically simple. Moreover,*

$$\begin{cases} r(\mathcal{K}_{\theta,s}) \le c^{(\sigma_n - s)/(\sigma_n - a)} < 1, & a < s < \sigma_n, \\ r(\mathcal{K}_{\theta,s}) \ge c^{-(s-\sigma_n)/(\sigma_n - a)} > 1, & \sigma_n < s < a + 1. \end{cases} \tag{5.1}$$

Proof sketch. If $r(\mathcal{K}_{\theta,s}) > 1$ for $n/2 < s < \sigma_n$, Proposition 4.1 supplies a strictly positive left Perron eigenfunctional ℓ. Pairing (4.3) with it gives

$$(1 - r(\mathcal{K}_{\theta,s}))\ell(\Phi_s) = \ell(\Theta_{\theta,s}) \ge 0,$$

a contradiction. If $I - \mathcal{K}_{\theta,\sigma_n}$ were invertible, norm continuity and the bounded inhomogeneous term would bound Φ_s near σ_n, contradicting (4.4). Thus one is in the spectrum. Persistence of isolated eigenvalues excludes a larger spectral radius there, giving $r(\mathcal{K}_{\theta,\sigma_n}) = 1$.

After radial disintegration of the positive measure μ_n, Hölder's inequality gives log-convexity of the spectral radius in s. Log-convexity and the bound at a give (5.1). The positive density in Proposition 4.1 gives a one-dimensional eigenspace at eigenvalue one. Pairing with the positive left eigenfunctional excludes a generalized eigenvector outside that eigenspace. Thus the eigenvalue is algebraically simple, and its analytic branch ϱ_θ satisfies

$$\varrho'_\theta(\sigma_n) \ge \frac{-\log c_\theta}{\sigma_n - a_\theta} > 0. \tag{5.2}$$

In particular $(I - \mathcal{K}_{\theta,z})^{-1}$ has a simple pole at σ_n. □

Proof sketch of [Cai26, Theorem 1.4]. Set $\beta_n = 2\sigma_n - n \in (0,1)$. The conjugacy (4.1) and Proposition 5.1 give $r(\mathcal{L}_{n,\beta_n}) = 1$ and algebraic simplicity. For $\beta \geq \beta_n$, the prescribed weight satisfies $\theta_\beta < (n+3)/2 - \sigma_n$, so (5.1) gives the strict inequality above β_n. Below β_n, apply the same proposition if σ_n lies in the strip for θ_β. Otherwise choose $s(\beta) < t < \min(\sigma_n, a_{\theta_\beta} + 1)$; Proposition 4.2 gives spectral radius at most one at t, and interpolation from a_{θ_β} gives a strict bound below one at $s(\beta)$. Here $c_{\theta_\beta} = 3/(4\cos^2(\pi\beta/6)) < 1$. Thus β_n is the unique root, and $\sigma_n^2 = 1/4 + 3\xi_n$ gives [Cai26, (1.7)]. □

References

[BN11] V. Beffara and P. Nolin, *On monochromatic arm exponents for 2D critical percolation*, Ann. Probab. **39** (2011), no. 4, 1286–1304.

[Cai26] G. Cai, *Monochromatic arm exponents for critical planar percolation.*

[DMMY26] I. Đanković, M. Markering, J. Miller, and Y. Yuan, *The scaling limit of random walk and the intrinsic metric on planar critical percolation*, preprint, arXiv:2604.14122v1 (2026).

[GM18] E. Gwynne and J. Miller, *Chordal* SLE_6 *explorations of a quantum disk*, Electron. J. Probab. **23** (2018), Paper No. 66, 24 pp.

[KKR13] A. Kuznetsov, A. E. Kyprianou, and V. Rivero, *The theory of scale functions for spectrally negative Lévy processes*, Lévy Matters II, Lecture Notes in Math., vol. 2061, Springer, 2013, pp. 97–186.

[Nol08] P. Nolin, *Near-critical percolation in two dimensions*, Electron. J. Probab. **13** (2008), no. 55, 1562–1623.

[RZ20] G. Rémy and T. Zhu, *The distribution of Gaussian multiplicative chaos on the unit interval*, Ann. Probab. **48** (2020), no. 2, 872–915.

[SW01] S. Smirnov and W. Werner, *Critical exponents for two-dimensional percolation*, Math. Res. Lett. **8** (2001), 729–744.

Beijing International Center for Mathematical Research, Peking University,
No.5 Yiheyuan Road, Haidian District, Beijing 100871, P.R.China
Email address: caigefei1917@pku.edu.cn